Ocean Science Journal, Vol. 42 No. 4, 199-209(2007)

Article

Ocean Science Journal

http://osj.kordi.re.kr

Comparison of Chlorophyll Algorithms in the Bohai Sea of China

Peng Xiu[1]*, Yuguang Liu[1], Zengrui Rong[1], Haibo Zong[1], Gang Li[3], Xiaogang Xing[1], and Yongcun Cheng[1,2]

[1]*College of Physical and Environmental Oceanography, Physical Oceanography Laboratory, Ocean University of China, Qingdao 266100, China*

[2]*Institute of Meteorology, PLA University of Science and Technology, Nanjing 211101, China*

[3]*Shenzhen Key Laboratory for Coastal and Atmospheric Research, Pku-hkust Shenzhen-hongkong Institution, Shenzhen 518057, China*

Received 13 July 2007; Revised 3 September 2007; Accepted 17 October 2007

Abstract – Empirical band-ratio algorithms and artificial neural network techniques to retrieve sea surface chlorophyll concentrations were evaluated in the Bohai Sea of China by using an extensive field observation data set. Bohai Sea represents an example of optically complex case II waters with high concentrations of colored dissolved organic matter (CDOM). The data set includes coincident measurements of radiometric quantities and chlorophyll a concentration (Chl), which were taken on 8 cruises between 2003 and 2005. The data covers a range of variability in Chl in surface waters from 0.3 to 6.5 mg m^{-3}. The comparison results showed that these empirical algorithms developed for case I and case II waters can not be applied directly to the Bohai Sea of China, because of significant biases. For example, the mean normalized bias (MNB) for OC4V4 product was 1.85 and the root mean square (RMS) error is 2.26.

Key words – chlorophyll concentration, ocean color, remote sensing model, case II waters, Artificial Neural Network

1. Introduction

Satellite ocean color research began in the late 1970s with the coastal zone color scanner (CZCS) aboard the Nimbus 7 satellite which acquired data from October 1978 to June 1986 (Evans and Gordon 1994; Acker 1994). Since then, significant efforts have been made to develop ocean color satellite missions with improved spectral and radiometric performance, spatial and temporal coverage, and quality of data products (Morel 1998). These efforts have resulted in the Sea-viewing Wide Field-of-view Sensor (SeaWiFS) (Hooker and McClain 2000), launched on the OrbView-2 spacecraft in August 1997, and the Moderate Resolution Imaging Spectroradiometers (MODIS) (Esaias *et al.* 1998), launched on the NASA Earth Observing System (EOS) satellites Terra and Aqua in December 1999 and May 2002, respectively.

Satellite ocean color data provides a practical means for monitoring the spatial and seasonal variation of near surface information for the study of oceanic primary production, global carbon and other biological cycles. The influence of phytoplankton on the ocean color of seawater has been studied for several decades. It is well understood that chlorophyll a (Chl), the primary photosynthetic pigment in phytoplankton, absorbs relatively more blue and red light than green, and the spectrum of backscattered sunlight progressively shifts from deep blue to green as the concentration of phytoplankton increases (O' Reilly *et al.* 1998). In case I waters, substances other than phytoplankton are either optically insignificant or correlated with phytoplankton. The case I water assumptions imply that the ocean optical properties can be modeled as a function of chlorophyll concentration alone, which has led to algorithms for retrieving phytoplankton pigments from remotely sensed ocean color. The current satellite operational algorithms for retrieval of pigments and other bio-optical properties have been empirically derived from field data collected mainly in ocean waters that are assumed to be case I (*e.g.* O'Reilly *et al.* 1998, 2000). According to a bipartite classification scheme, optically complex waters that cannot be classified as case I are designated as case II waters. Typically, case II waters include coastal and inland water bodies where

*Corresponding author. E-mail: xiupeng1015@yahoo.com.cn

agents other than phytoplankton such as suspended inorganic particles and/or dissolved organic matter (and perhaps even a bottom reflectance) make a significant contribution to the optical properties (*e.g.* Bukata *et al.* 1995; Sathyendranath 2000). It is well recognized that case II waters require new algorithms based on new approaches for dealing with both atmospheric correction and retrievals of ocean bio-optical properties from water-leaving radiance (Sathyendranath 2000). Therefore, it is useful to develop an understanding of limitations and to quantify errors of current standard algorithms in various case II waters, especially as no specific algorithms exist that would allow masking of regions where case I algorithms may not hold.

The Bohai Sea of China is a semi-enclosed sea with a typical case II water environment, located at the northernmost end of eastern Chinese mainland between 37°07′~41°N and 117°35′~122°15′E (see Fig. 1). Case II waters in the Bohai Sea are often dominated by colored dissolved organic matter (CDOM). Large discharges from rivers and a relatively shallow sea floor significantly influence the optical properties. Studies showed that subsurface chlorophyll maximum concentration also has a significant effect on sea surface chlorophyll concentration (Xiu and Liu, 2006; Xiu *et al.* 2007). Thus, a comprehensive analysis of the performance of empirical algorithms that are based on the blue-green bands should be beneficial for the current use of remote sensing and for future efforts on algorithm development.

2. Materials and Methods

The validation of six bio-optical algorithms and one Artificial Neural Network (ANN) algorithm (see Appendix A and figure 9) was carried out with field data collected on 8 cruises between 2003 and 2005 (Table 1). The data were collected under various environmental conditions. The spatial coverage includes very turbid waters in the mouth

Table 1. The list of cruises and the number of optical measurements made in each cruise

Cruise	Date	Measured Chl and R_{rs}
1	March 21-March 23, 2003 April	13
2	19-April 25,2003	7
3	June 18-June 26, 2003	41
4	July 13-July 15, 2003	7
5	August 12-August 26, 2003	42
6	August 9-August 22, 2004	30
7	June 6-June 18, 2005	48
8	August 23-September 1, 2005	44

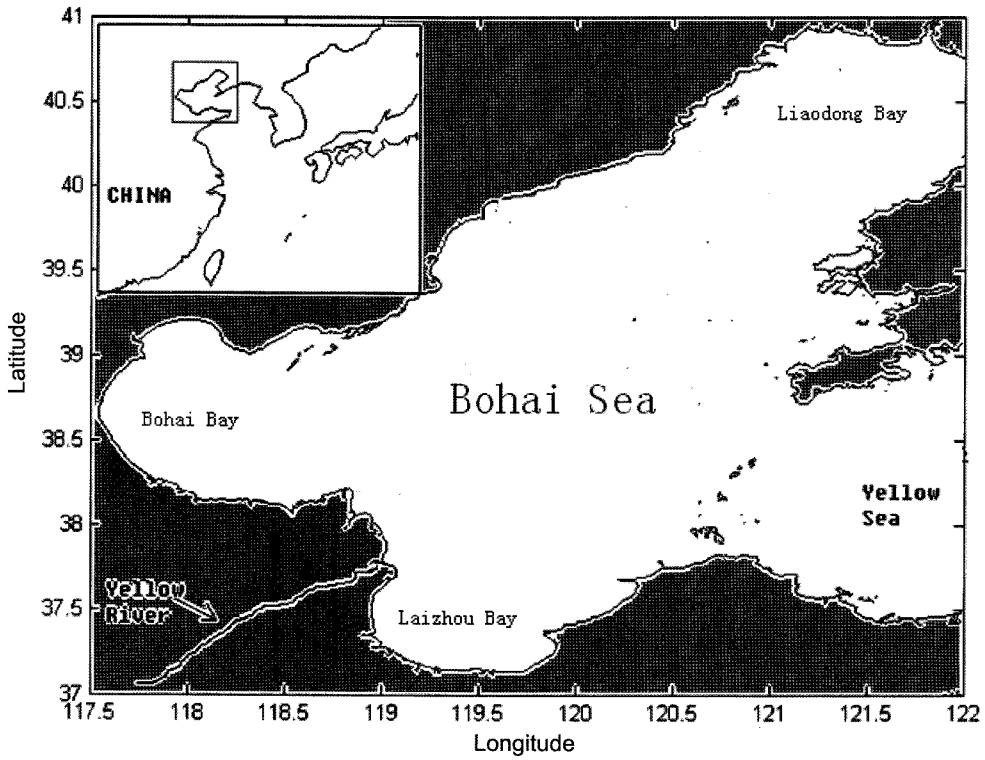

Fig. 1. Map of the Bohai Sea, showing major geographical features.

area of Yellow river; less turbid coastal waters and relative clear water further away from the coast and in the central Bohai.

Radiometric measurements

The spectral remote-sensing reflectance ($R_{rs}(\lambda)$) and normalized water-leaving radiance ($L_{wn}(\lambda)$) were calculated by above-water measurements. Briefly, multiple spectra of above-surface upwelling radiance (L_u) and downwelling sky radiance (L_{sky}) were collected by using a 256-channel spectroradiometer with wavelengths ranging from 365 to 1070 nm. The water-leaving radiance was then calculated by subtracting from the total upwelling radiance the portion of the skylight reflected into the sensor along with any solar glint (Lee *et al.* 1996):

$$L_w(\lambda) = L_u(\lambda) - r(i)L_{sky}(i) - \Delta E_d \quad (1)$$

where i is the zenith angle, $r(i)$ is the Fresnel reflectance. For open ocean, ΔE_d, a solar glint correction, is estimated by assuming $L_w(750)=0$; For coastal waters, ΔE_d is estimated iteratively without assuming $L_w(750)=0$ (Lee and Carder 2004). We measured spectra L_u and L_{sky} three times respectively, and in order to obtain L_w, the averaged spectra of L_u and L_{sky} were used in order to decrease random measurement errors (Lee *et al.* 1996).

Using the measured radiance (L_G) normal to a standard diffuse reflectance panel, the total downwelling irradiance E_d is determined by

$$E_d(\lambda) = \frac{\pi L_G(\lambda)}{R_G(\lambda)} \quad (2)$$

where R_G is the reflectance of the diffuse panel, whose value is about 25% used in our experiments. Then spectral remote-sensing reflectance and normalized water-leaving radiance was obtained by

$$R_{rs}(\lambda) = \frac{L_w(\lambda)}{E_d(\lambda)} \quad (3)$$

$$L_{wn}(\lambda) = F_0(\lambda)R_{rs}(\lambda) \quad (4)$$

where $F_0(\lambda)$ is the mean extraterrestrial solar irradiance at a given spectral band.

Chlorophyll a measurements

On all cruises, the chlorophyll *a* concentration was determined using the spectrophotometric method. The samples of surface water were filtered under low pressure (less than 0.5 atm) using Whatman glass-fiber filters (GF/F 47 mm in diameter) as soon as possible after collection. The particulate matter retained on the filters was extracted for a 24 hour in 96% ethanol. The absorbance of the extract was then measured on a specific spectrophotometer. With the measured absorbance, chlorophyll concentrations were then converted by (Darecki and Stramski 2004).

Evaluation criteria

We will now evaluate the performance of six ocean color algorithms in the Bohai Sea using measured $R_{rs}(\lambda)$ and $L_{wn}(\lambda)$ as inputs (shown in Appendix A). The evaluation process is based on a comparison of the algorithm-derived values of the pigment concentration with the field observations. The mean normalized bias (MNB) (systematic error) and the normalized root mean square (RMS) error (random error) are defined as follows:

$$MNB = mean\left(\frac{y_{alg} - y_{obs}}{y_{obs}}\right) \quad (5)$$

$$RMS = sta\left(\frac{y_{alg} - y_{obs}}{y_{obs}}\right) \quad (6)$$

where y_{alg} is chlorophyll concentration estimated from the algorithm, y_{obs} is the observed value, and 'mean' and 'std' indicate the calculations of mean and standard deviation values, respectively:

$$mean(\chi) = \bar{\chi} = \frac{1}{N}\sum_{i=1}^{n}\chi_i \quad (7)$$

$$sta(\chi) = \left[\frac{1}{n-1}\sum_{i=1}^{n}(\chi_i - \bar{\chi})^2\right]^{1/2} \quad (8)$$

where χ is the variable of interest. We also used the statistics based on root mean square of the logarithm of the ratio of algorithm-derived to measured values. Such statistics can provide a good measure of data scatter for lognormally distributed variables, which are often observed for chlorophyll data sets. These errors are calculated from the following equations

$$\log\_bias = mean\left(\log\left(\frac{y_{alg}}{y_{obs}}\right)\right) \quad (9)$$

$$\log\_rms = std\left(\log\left(\frac{y_{alg}}{y_{obs}}\right)\right) \quad (10)$$

3. Results and Discussions

Fig. 2 shows the frequency distribution of chlorophyll concentration based on our entire data set. From this histogram we can see that the range of concentration is approximately from 0.3 to 6.5 mg m^{-3}, and chlorophyll values between 0.3 and 1.05 mg m^{-3} occur most frequently.

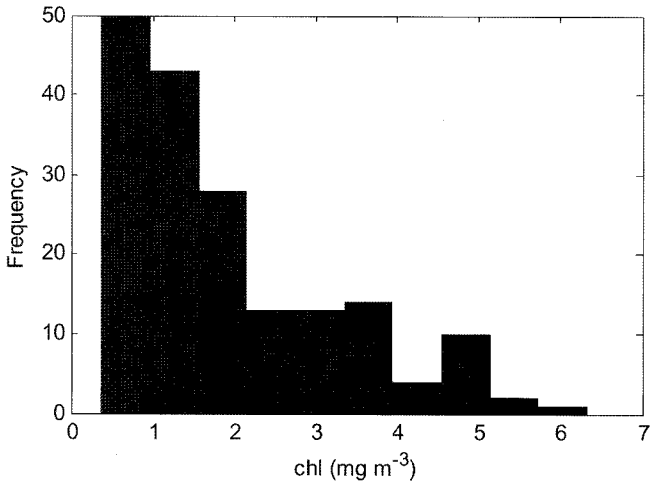

Fig. 2. Frequency distribution of chlorophyll concentration based on our entire data set; the ticks of the y-axis denote the number of investigation sites.

Comparisons of measured and the six algorithm-derived estimates of chlorophyll concentrations are presented in Figs. 3-8. Fig. 3a shows the CZCS_pigm comparison result. The underestimation data points (60%) and overestimation data points (40%) spread almost equally around the 1:1 line. The CZCS_pigm algorithm gives in many cases very high relative errors, some of which are often unrealistically high as is shown in Fig. 3b. The highest relative error is 1000%, and there are about 19% stations where the relative errors are higher than 100%. Except for the highest relative error, the other errors continuously decrease from about 600%. The correlation coefficient between retrieved and measured chlorophyll concentration is 0.20; the MNB and RMS error are 0.42 and 1.57 respectively. The log_bias is -0.029 and log_rms is 0.81. Fig. 3c shows the geographical positions of our investigation sites. Apparently, stations with high relative errors lie most in the Bohai Bay, Laizhou Bay and Yellow River area. The high errors are mainly due to the high concentrations of the suspended particulate matter brought by the inputs of the Yellow River. We can see that there is a good regression relationship between these high

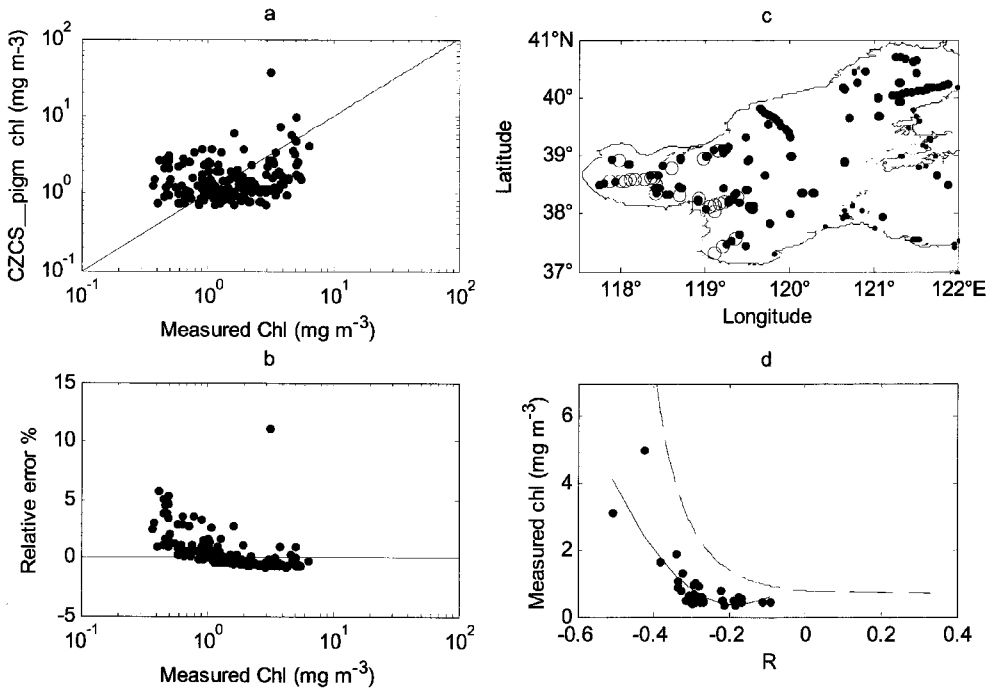

Fig. 3. Comparison results of CZCS_pigm algorithm. (a) Statistical relationship between measured chlorophyll concentration and CZCS_pigm results. (b) Relative errors. (c) Geographical positions of our investigation sites, in which points denoted by circles are where relative errors are higher than 100%. d) Statistical relationship between the measured Chl and R in the area where relative errors are higher than 100%; the solid curve is the polynomial regression curve and the dashed curve is the standard CZCS_pigm curve.

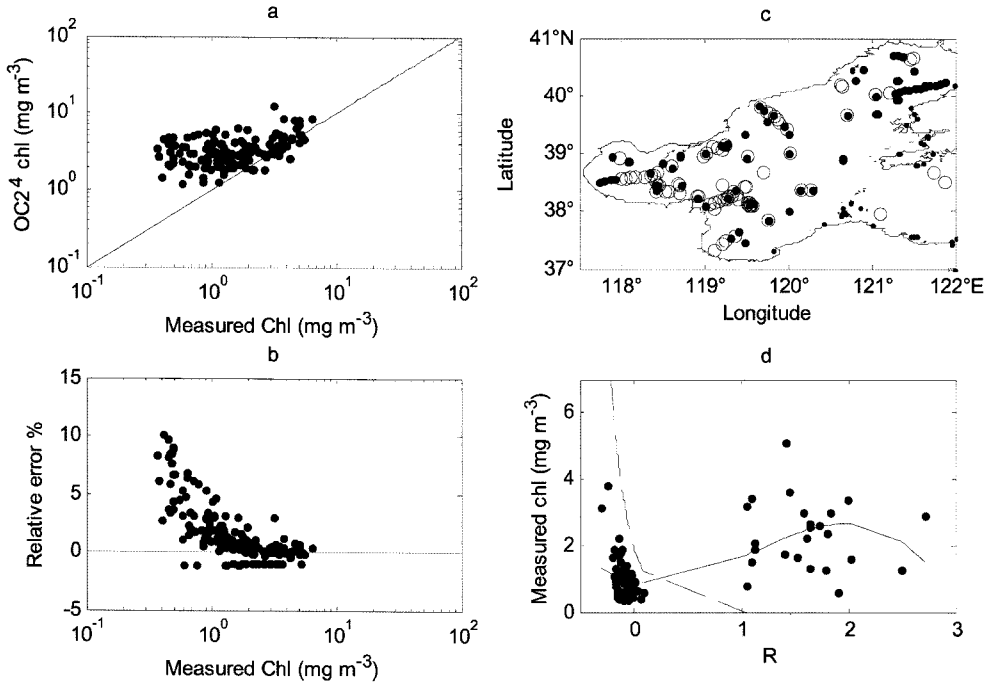

Fig. 4. Comparison results of SeaWiFS OC2v4 algorithm. (a) Statistical relationship between measured chlorophyll concentration and OC2v4 results. (b) Relative errors. (c) Geographical positions of our investigation sites, in which points denoted by circles are where relative errors are higher than 100%. (d) Statistical relationship between the measured Chl and R in the area where relative errors are higher than 100%; the solid curve is the polynomial regression curve and the dashed curve is the standard OC2v4 curve.

error points (Fig. 3d), and the correlation coefficient is 0.79; the MNB and normalized RMS error are 0.14 and 0.44 respectively.

Fig. 4 shows the comparison results between SeaWiFS algorithm OC2v4 derived chlorophyll concentrations and measured values. As we can see, most of the derived values (79%) show overestimations. The highest relative error is 1013% and from which the relative error continuously decreases. There are about 57% stations where relative errors are higher than 100%. Correlation coefficient between retrieved and measured chlorophyll concentration is 0.30; MNB and RMS error are 1.56 and 2.45 respectively. The log_bias is 0.83 and log_rms is 0.69 (Figs. 4a, b). It is also indicated that data points with high errors (relative errors >100%) spread in almost the entire Bohai Sea, and low errors only occur in the Liaodong Bay area (Fig. 4c). However, we can not obtain a good polynomial regression relationship between these two types of data (Fig. 4d); the correlation coefficient between them is 0.62; the MNB and the normalized RMS error are 0.28 and 0.65 respectively.

Performance of SeaWiFS OC4v4 in the Bohai Sea is shown in Fig. 5. The result shows an obvious overestimation (about 90% data points in all) of the real chlorophyll concentrations. The highest relative error is 956% and from which the relative error continuously decreases. There are about 49% stations where relative errors are higher than 100%. Correlation coefficient between retrieved and measured chlorophyll concentration is 0.48; the MNB and the normalized RMS error are 1.85 and 2.26, respectively. The log_bias is 0.79 and log_rms is 0.70. Like CZCS algorithm, high error data points mostly exist in the Bohai Bay, Laizhou Bay and especially in the Yellow River area (Fig. 5c). In figure5d, the shape of the regression curve is quite like standard OC4v4 curve. Correlation coefficient between the measured and derived concentrations is 0.60, and the MNB and the normalized RMS error are 0.23 and 0.59 respectively.

Performance of the MODIS case I water algorithm chlor_MODIS in the Bohai Sea is shown in Fig. 6. Like CZCS algorithm, the underestimation data points (54%) and overestimation data points (46%) spread almost equally around the 1:1 line. The highest relative error is 990.1%, and there are about 22% stations where relative errors are higher than 100%. Except for the highest relative error, the other errors continuously decrease from about 600%. Correlation coefficient between retrieved and the measured

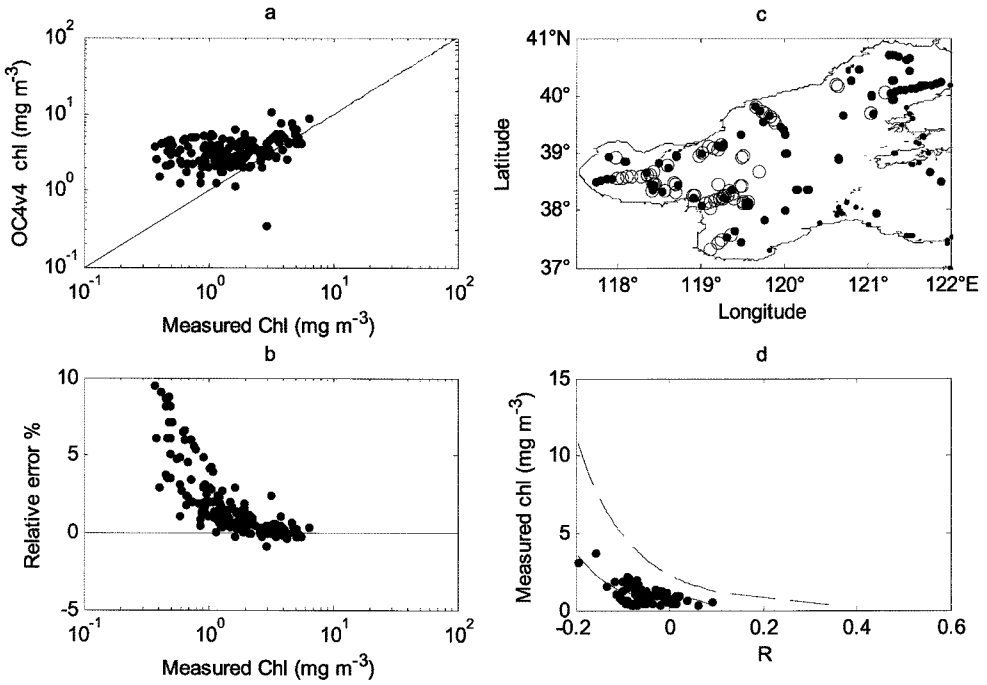

Fig. 5. Comparison results of SeaWiFS OC4v4 algorithm. (a) Statistical relationship between measured chlorophyll concentration and OC4v4 results. (b) Relative errors. (c) Geographical positions of our investigation sites, in which points denoted by circles are where relative errors are higher than 100%. (d) Statistical relationship between the measured Chl and R in the area where relative errors are higher than 100%; the solid curve is the polynomial regression curve and the dashed curve is the standard OC4v4 curve.

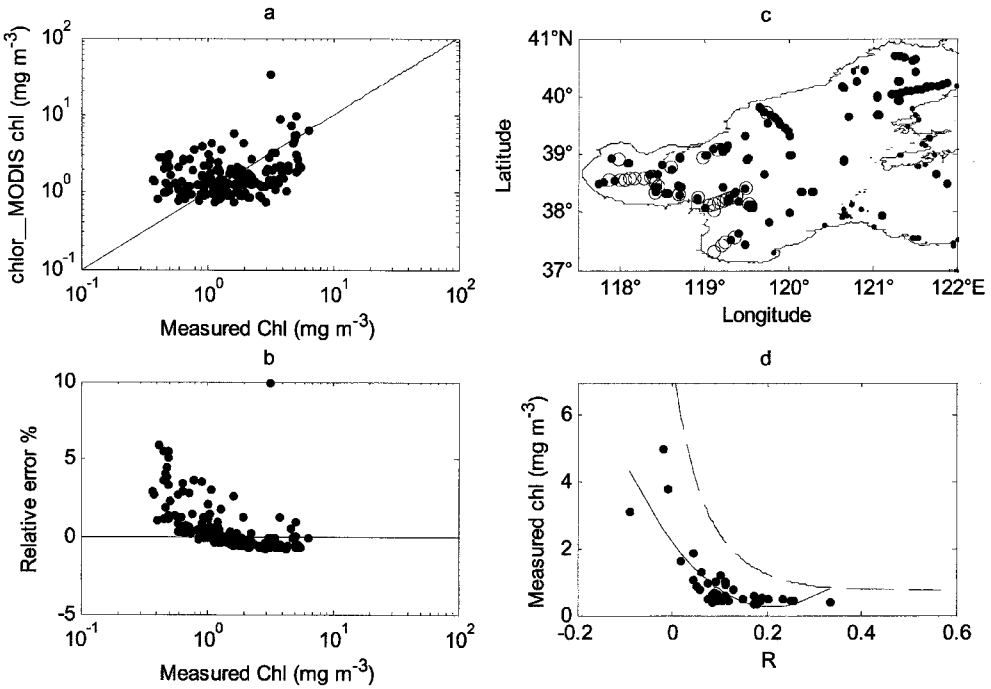

Fig. 6. Comparison results of MODIS case I chlor_MODIS algorithm. (a) Statistical relationship between measured chlorophyll concentration and chlor_MODIS results. (b) Relative errors. (c) Geographical positions of our investigation sites, in which points denoted by circles are where relative errors are higher than 100%. (d) Statistical relationship between the measured Chl and R in the area where relative errors are higher than 100%, the solid curve is the polynomial regression curve and the dashed curve is the standard chlor_MODIS curve.

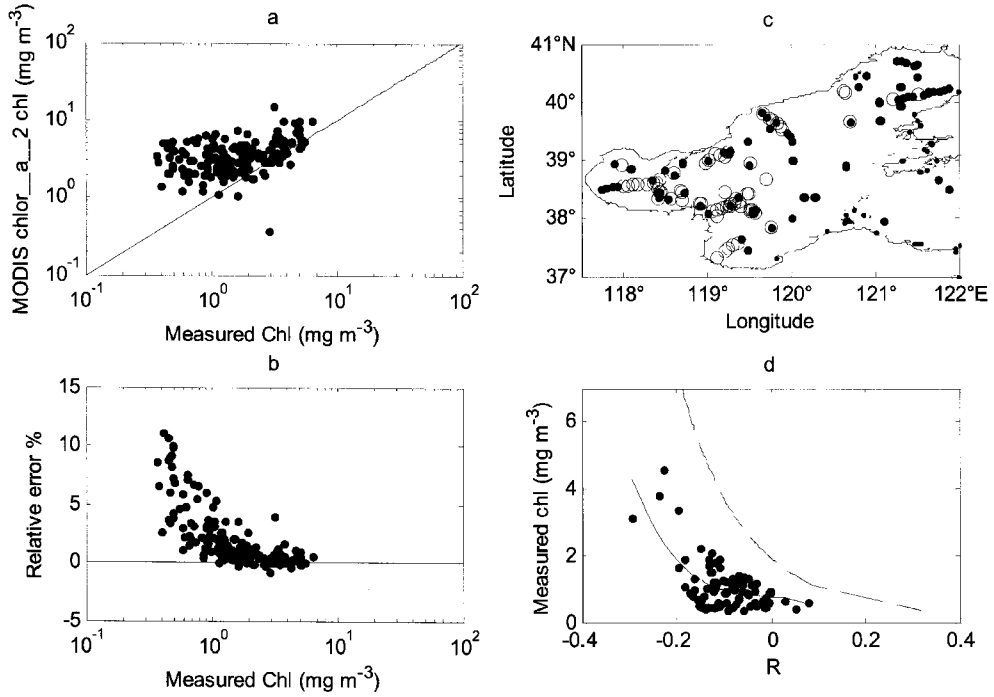

Fig. 7. Comparison results of MODIS case II chlor_a_2 algorithm. (a) Statistical relationship between measured chlorophyll concentration and chlor_a_2 results. (b) Relative errors. (c) Geographical positions of our investigation sites, in which points denoted by circles are where relative errors are higher than 100%. (d) Statistical relationship between the measured Chl and R in the area where relative errors are higher than 100%; the solid curve is the polynomial regression curve and the dashed curve is the standard chlor_a_2 curve.

chlorophyll concentration is 0.27, the MNB and the normalized RMS error are 0.50 and 1.53 respectively. The log_bias is 0.07 and log_rms is 0.77. Also, most of the large error data points exist in the Bohai Bay, Laizhou Bay and the Yellow River area (Fig. 6c). Correlation coefficient of the data points where relative errors are higher than 100% is 0.80, and the MNB and the normalized RMS error are 0.14 and 0.54 respectively (Fig. 6d).

Performance of the MODIS case II water algorithm chlor_a_2 in the Bohai Sea is shown in Fig. 7. The result shows an obvious overestimation (about 99% data points of all) of the real chlorophyll concentrations. The highest relative error is 1112% and from which the relative error continuously decreases. There are about 49% stations where relative errors are higher than 100%. Correlation coefficient between retrieved and measured chlorophyll concentration is 0.48, the MNB and the normalized RMS error are 1.95 and 2.48, respectively. The log_bias is 0.81 and log_rms is 0.72. Most of the large error data points exist in the Bohai Bay, Laizhou Bay and the Yellow River area (Fig. 7c). The correlation coefficient of the data points that relative errors are higher than 100% is 0.66, and the MNB and the normalized RMS error are 0.25 and 0.62 respectively (Fig. 7d).

Tang's model (Tang *et al.* 2004) chlor_t algorithm is a regional model derived from the in-situ observations in the south Yellow Sea and East China Sea. This algorithm was also tested here, because it is suitable for chlorophyll retrieval in China seas. Using this algorithm in the Bohai Sea, we also obtained an obvious overestimation (about 80% data) of the real chlorophyll concentration. The highest relative error is 478% and from which the relative error continuously decreases. There are about 34% stations where relative errors are higher than 100%. Correlation coefficient between retrieved and measured chlorophyll concentration is 0.66; the MNB and the normalized RMS error are 1.00 and 1.22 respectively. The log_bias is 0.53 and log_rms is 0.57. Different from above algorithms, high error data points exist only in the Bohai Bay and the Yellow River area (Fig. 8c). We also can get a good regression relationship (correlation coefficient is 0.86) between R and measured Chl of the data points where relative errors are higher than 100%. The MNB and the normalized RMS error are 0.09 and 0.34 respectively (Fig. 8d).

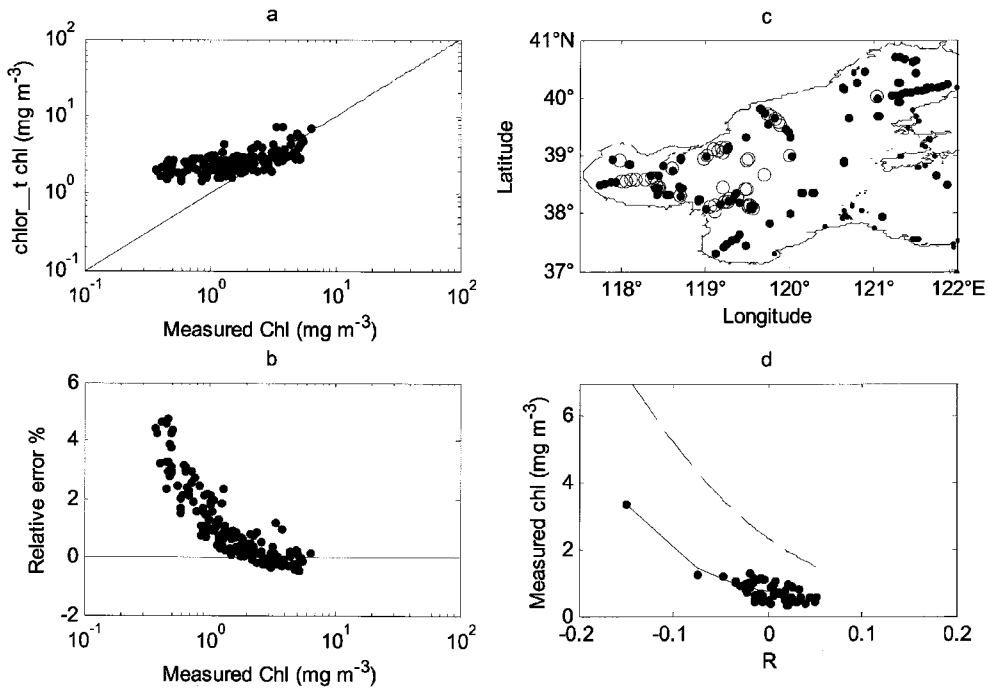

Fig. 8. Comparison results of chlor_t algorithm which was derived from the in-situ observations in China seas. (a) Statistical relationship between measured chlorophyll concentration and chlor_t results. (b) Relative errors. (c) Geographical positions of our investigation sites, in which points denoted by circles are where relative errors are higher than 100%. (d) Statistical relationship between the measured Chl and R in the area where relative errors are higher than 100%; the solid curve is the polynomial regression curve and the dashed curve is the standard chlor_t curve.

In addition to the band-ratio algorithms, we also tested the performance of the Artificial Neural Network (ANN) techniques to retrieve sea surface chlorophyll concentrations in the Bohai Sea. Neural networks were originally developed to model the functioning of the human brain. They have applications in the fields of classification, pattern recognition, and signal processing. A complete introduction to the different types of neural networks and their applications can be found in Wasserman (1989), Beale and Jackson (1990), Dayhoff (1990), and Masters (1993; 1995) *et al.* It has been recognized that artificial neural network techniques also have a good potential to derive the water constituents both in case I and case II waters (Schiller and Doerffer 1999). Gross *et al.* (2000) have shown that noise from radiometric performance, imperfect atmospheric correction, and the passage from bi-directional reflectance can be more effectively filtered out of data from case I water with a forward-feed, back propagating neural network. Furthermore, Keiner and Brown (1999) produced an improved chlorophyll algorithm by applying a similar ANN to a data set of ship-based reflectances at the same spectral bands as SeaWiFS data in predominately case I waters. Also, past research has shown that satellite ocean color data, in conjunction with a neural network, can be used to effectively discern several water constitutes, including chlorophyll concentration, suspended sediment, and gelbstoff and also can be used to correct for imperfect atmospheric correction in case II waters (Zhang *et al.* 2003; Baruah *et al.* 2000; Keiner and Yan 1998). In the present study, we proposed a multi-layer, feedforward type, and error backpropagation neural network (Fausset 1994. see figure9). This network consists of an input layer, one hidden layer, and an output layer. Each layer is connected by a series of weights. These weights are simply variables. Their collective purpose is to act as memory for the system. When a network learns to map an input to an output vector, this mapping is contained in the weights. The number of hidden layer nodes needed depends on the complexity of the function to be approximated.

In this study, input to the network is diffuse remote-sensing reflectance just above the sea surface, and output is the concentration of sea surface chlorophyll. Field data in the Bohai Sea were divided into two parts, one was used as the training data set (70% data), and the other was used as the validation data set (30% data). To determine which and

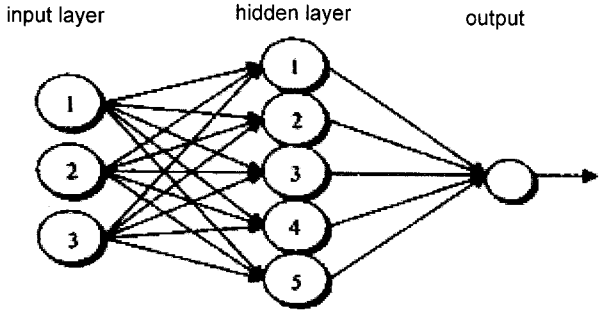

Fig. 9. The structure of simplified artificial neural network.

how many spectral bands or band ratios are best for pigment retrieval, several combinations of input data were tested. Another important factor influencing the performance of the ANN is the number of hidden neurons used. Generally speaking, if too few hidden neurons are used, high training error and high generalization error may be obtained due to underfitting and high statistical bias. If too many hidden neurons are used, low training error may result, but there may be high generalization errors due to overfitting and high variance. Overfitting is a situation where the network correctly learns not only the correct pattern, but also the noise in the inputs, resulting in poor performance when network is applied to real problems (Krasnopolsky *et al.* 1995). So, we tested the number of neurons from 4 to 30.

After experimentation, Fig. 10 shows our best combination of ANN with remote-sensing reflectance at band 412, 443, 490, 510, 555, 670, 700, and 720 as the inputs; the number of the hidden neurons is 5. For the validation data set, correlation coefficient between the log-transformed ANN derived-concentration and measured is 0.94 and RMS is 0.083. However, during our model training, the phenomena of overfitting always occur. It is very difficult to get a good result with low RMS. Sometimes we can get low RMS for the training data, but with very high RMS for the validation data. When we apply this well-trained and validated network in some our newly measured data, the retrieval result is quite poor (correlation coefficient is 0.32). The reason for this may be due to the complicated relationship between remote-sensing reflectance and sea surface chlorophyll concentration caused by the high concentrations of suspended particular matter and color dissolved organic matter or the bottom effect.

4. Conclusions

We tested the performance of six empirical band-ratio algorithms and one ANN technique to retrieve sea surface chlorophyll concentration using an extensive bio-optical data set collected on 8 cruises between 2003 and 2005. Our analysis revealed a systematic and large overestimation or underestimation of chlorophyll products by using some algorithms designed for case II waters. It appears that the Bohai Sea requires new approaches and new parameterizations

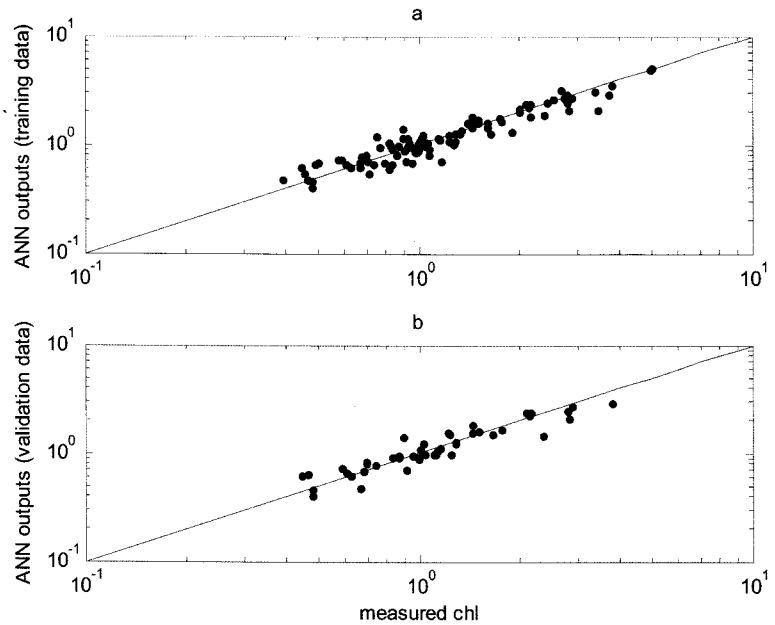

Fig. 10. Scatter plot of the ANN derived chlorophyll concentration with the measured concentration.

for both empirical and semi-analytical pigment algorithms. High concentrations of CDOM, detritus, and suspended particulate matters caused by large riverine discharges or local wind-induced vertical mixing all contribute to the failure of pigment algorithms. Also, since the average depth in the Bohai Sea is only 18 meters, ocean bottom effect may be a large source of retrieval errors.

For the present operational pigment algorithms, it seems that CZCS_pigm and chlor_MODIS algorithms have higher accuracy over the entire Bohai Sea region. Surprisingly, both of the algorithms use normalized water-leaving radiance as an input factor. The reason for this may be due to the field measurement carried out just above sea surface but not from the space. OC4V4 and chlor_a_2 algorithms have moderate ability in pigment retrieval, and OC2V4 algorithm is the worst one. Specifically, CZCS_pigm and chlor_MODIS work well in Liaodong Bay and the central region. The regional model chlor_t works well in Laizhou Bay. OC2V4, OC4V4 and chlor_a_2 seem to be better in the Bohai Bay than CZCS_pigm and chlor_MODIS, but none of them is acceptable, and further investigation is needed.

Acknowledgement

This work is supported by Special Funds for Major State Basic Research Project under Grant No. 973-2007CB411807 and the National High Technology Development Project of China under Grant No. 863-2006AA09Z140.

References

Acker, J.G. 1994. The heritage of SeaWiFS: A retrospective on the CZCS NIMBUS Experiment Team (NET) Program, NASA. p. 44. In: *The Memo,* ed. by S. B. Hooker and E. R. Firestone. NASA Gorddard Space Flight Cent., Greenbelt, MD.

Beale, R. and T. Jackson. 1990. Neural Computing: An Introduction. Adam Hilger, Bristol, UK.

Baruah, P.J., K. Oki., and H. Nishimura. 2000. A neural network model for estimating Surface Chlorophyll and Sediment Content at the Lake Kasumi Gaura of Japan. Proceedings of 21st Asian Conference of Remote Sensing, Taipei, Taiwan.

Bukata, R.P., J.H. Jerome, K. Ya. Kondratyev, and D.V. Pozdnyakov. 1995. Optical properties and remote sensing of inland and coastal waters. CRC Press, Boca Raton.

Clark, D.K. 1997. MODIS Algorithm Theoretical Basis Document, Bio- Optical lgorithms—Case 1 Waters, version 1.2, Available from WWW: <http://modis.gsfc.nasa.gov/data/atbd/atbd_mod18.pdf>

Dayhoff, J. 1990. Neural Network Architectures: An Introduction. Van Nostrand Reinhold, New York.

Darecki, M., and D. Stramski. 2004, An evaluation of MODIS and SeaWIFS bio-optical algorithms in the Baltic Sea. *Remote Sens. Environ.*, **89**, 326-350.

Esaias, W.E., M.R. Abbott, I. Barton, O.B. Brown, J.W. Campbell, K.L. Carder, D.K. Clark, R.H. Evans, F.E. Hoge, H.R. Gordon, W.M. Balch, R. Letelier, and P.J. Minnett. 1998. An overview of MODIS capabilities for ocean science observations. *IEEE Trans. Geosci. Remote Sens.*, **36**, 1250-1265.

Evans, R.H. and H.R. Gordon. 1994. CZCS system calibration: A retrospective examination. *J. Geophys. Res.*, **99**, 7293-7307.

Fausett, L. 1994. Fundamentals of neural networks: Architectures, Algorithms, and Applications. Prentice Hall, Englewood Cliffs, N.J.

Gross, L., S. Thiria, R. Frouin, and B.G. Mitchell. 2000. Artificial neural networks for modeling the transfer function between reflectance and phytoplankton pigment concentration. *J. Geophys. Res.*, **106**, 3483-3495.

Hooker, S.B. and C.R. McClain. 2000. The calibration and validation of SeaWiFS data. *Prog. Oceanogr.*, **45**, 427-465.

Keiner, L.E. and X.H. Yan. 1998. A neural network model for estimating sea surface chlorophyll and sediments from thematic mapper imagery. *Remote Sens. Environ.*, **66**(2), 153-165.

Keiner, L.E. and C.W. Brown. 1999. Estimating oceanic chlorophyll concentrations with neural networks. *Int. J. Remote Sens.*, **20**, 189-194.

Krasnopolshy, V., L. Breaker, and W. Gemmil. 1995. A neural network as a nonlinear transfer model for retrieving surface wind speeds from the special sensor microwave imager. *J. Geophys. Res.*, **100**, 11033-11045.

Lee, Z.P., K.L. Carder, R.G. Steward, T.G Peacock, C.O. Davis, and J.L. Mueller. 1996. Remote-sensing reflectance and inherent optical properties of oceanic waters derived from above-water measurements. *Proc. SPIE (Ocean Optics XIII)*, **2963**, 160-166.

Lee, Z.P. and K.L Carder. 2004. Absorption spectrum of phytoplankton pigments derived from hyperspectral remote-sensing reflectance. *Remote Sens. Environ.*, **89**, 361-368.

Masters, T. 1993. Practical Neural Network Recipes in C ++. Academic, San Diego, CA.

Masters, T. 1995. Advanced Algorithms for Neural networks: A C++ Sourcebook. Wiley, NewYork.

Morel, A. 1998. Minimum requirements for an operational ocean-colour sensor for the open ocean. IOCCG Report, vol. 1. Dartmouth, Nova Scotia, IOCCG Project Office. 46 p.

O'Reilly, J.E, S. Maritorena, B.G. Mitchell, D.A. Siegel, K.L. Carder, S.A. Garver, M. Kahru, and C. McClain. 1998. Ocean color chlorophyll a algorithms for SeaWIFS. *J. Geophys. Res.,*

103(C11), 24937-24953.

O'Reilly, J.E., S. Maritorena, D.A. Siegel, M.C. O'Brien, D. Toole, B.G. Mitchell, M. Kahru, F.P. Chavez, P. Strutton, G. Cota, S.B. Hokker, C.R. McClain, K.L. Carder, F. Muller-Karger, L. Harding, A. Magnuson, D. Phinney, G.F. Moore, J. Aiken, K.R. Arrigo, R. Letelier, and M. Culver. 2000. Ocean Color Chlorophyll a Algorithms for SeaWiFS, OC2 and OC4: Version 4. NASA Technical Memorandum 2000-206892, Vol. 11., NASA Goddard Space Flight Centre, Greenbelt, Maryland.

Schiller, H. and R. Doerffer. 1999. Neural network for emulation of an inverse model – operational derivation of Case II water properties from MERIS data. *Int. J. Remote Sens.*, **30**, 1735-1746.

Sathyendranath, S. 2000. Remote sensing of ocean colour in coastal, and other optically-complex, waters. IOCCG Report, vol. 3. Dartmouth, Nova Scotia, IOCCG Project Office. 140 p.

Tang, J. W., X.M. Wang, and Q.J. Song. 2004. The statistic inversion algorithms of water constituents for the Huanghai SeaandtheEastChinaSea.*ActaOceanol.Sin.*,**23**(4),617-626.

Wasserman, P. 1989. Neural Computing. Van Nostrand Reinhold, New York.

Xiu, P. and Y.G. Liu. 2006. Study on the correlation between chlorophyll maximum and remote sensing data. *J. Ocean Univ. China, Oceanic & Coastal Sea Res.*, **5**(3), 213-218.

Xiu, P., Y.G. Liu, and X.B. Yin. 2007. Preliminary study on distribution of deep chlorophyll maximum and remote sensing model in the Bohai Sea of China. *Int. J. Remote Sens.*, **28**(11), 2599-2612.

Zhang, T., F. Fell, Z.S. Liu, R. Preusker, J. Fischer, and M.X. He. 2003. Evaluating the performance of artificial neural network techniques for pigment retrieval from ocean color in Case I waters. *J. Geophys. Res.*, **108**, 3286-3298.

Appendix

Sensor	Identifier	Algorithm
CZCS	CZCS_pigm (Clark, 1997)	$CZCS\_pigm = 10^{(aR^3+bR^2+cR+d)/e)}$ $R = \log_{10}(L_{wn}(443)/L_{wn}(551))$ where if R>0.7368 a=-1.4443, b=1.4947, c=-2.5283, d=-0.0433, and e=1. if R>0.7368 a=-5.0511, b=2.8952, c=-0.5069, d=-0.11126, and e=1.
SeaWiFS	OC2V4 (O'Reilly *et al.* 1998).	$chl\_oc2 = e+10^{aR^3+bR^2+cR+d}$ $R = \log_{10}(R_{rs}(490)/R_{rs}(555))$ where a=-0.135, b=0.879, c=-2.336, d=0.319, and e=-0.071.
SeaWiFS	OC4V4 (O'Reilly *et al.* 2000).	$chl\_oc4 = e+10^{aR^4+bR^3+cR^2+dR+e}$ $R = \log_{10}\left(\frac{\max(R_{rs}(443)), R_{rs}(490), R_{rs}(510)}{R_{rs}(555)}\right)$ where a=-1.532, b=0.649, c=1.930, d=-3.076, and e=0.366.
MODIS	chlor_MODIS (Clark, 1997)	$chlor\_MODIS = 10^{(aR^3+bR^2+cR+d)/e}$ $R = \log_{10}(L_{wn}(443) + L_{wn}(488)) / L_{wn}(551)]$ where if R>0.9866 a=-2.8237, b=4.7122, c=-3.9110, d=0.8904, and e=1. if R>0.9866 a=-8.1067, b=12.0707, c=-6.0171, d=0.8791, and e=1.
MODIS	chlor_a_2 (O'Reilly *et al.* 2000).	$chl\_a\_2 = e+10^{aR^4+bR^3+cR^2+dR+e}$ $R = \log_{10}[\max(r_{25}, r_{35})]$ $r_{25} = R_{rs}(443)/R_{rs}(551)$ $r_{35} = R_{rs}(448)/R_{rs}(551)$ where a=-1.403, b=0.659, c=1.457, d=-2.753, and e=0.2830.
Regional model	chlor_t (Tang *et al.* 2004).	$chlor\_t = 10^{aR^2+bR+c}$ $R = \log_{10}\left[\frac{R_{rs}(443)R_{rs}(510)}{R_{rs}(555)R_{rs}(412)}\right]$ where a=-3.0679, b=-3.7278, and c=0.37457